Effects of microstructures on fatigue behavior of an Al-Mg-Sc alloy at an elevated temperature

doi: 10.4028/www.scientific.net/MSF.706-709.426

Effects of microstructures on fatigue behavior of an Al-Mg-Sc alloy at an elevated temperature

Chihiro Watanabe[1, a], and Ryoichi Monzen[1,b]

[1]Division of Innovative Technology and Science, Kanazawa University, Kakuma-machi, Kanazawa 920-1192, Ishikawa, Japan

[a]chihiro@t.kanazawa-u.ac.jp, [b]monzen@t.kanazawa-u.ac.jp

Keywords: Al-Mg-Sc alloy, Fatigue, Dislocation structure, Precipitation free zone

Abstract. Polycrystalline Al-1wt%Mg-0.27wt%Sc alloys bearing Al_3Sc particles with different average sizes of 4 and 11nm in diameter have been cyclically deformed at 423K under various constant stress amplitudes, and the relationship between fatigue characteristics and microstructure of the alloy has been investigated. The specimen bearing 11 nm particles exhibited a cyclic hardening to saturation, while in specimens with the small particles a cyclic softening was observed after initial hardening. In the specimen with large particles, dislocations were uniformly distributed under all applied stress amplitudes, whereas the specimens bearing small particles, in which cyclic softening occurred exhibited clearly developed slip bands. The cyclic softening for the latter specimen was explained by particle shearing within the strongly strained slip bands. The width of precipitate free zones (PFZs) has been found to be one of the factors affecting the fatigue life of the specimens at 423K. The two-step aging decreases the width of PFZs, resulting in increase in the fatigue life.

Introduction

Aluminum alloys with magnesium as the major alloying element constitute a group of non heat-treatable alloys with medium strength, high ductility, excellent corrosion resistance and weldability. Unfortunately, the strength of such Al-Mg alloys is lower than precipitation-hardening Al alloys. However, the addition of a small amount of scandium has been found to significantly improve the strength of Al-Mg alloys [1-3], owing to the presence of coherent, finely dispersed $L1_2$ Al_3Sc precipitate particles that can be obtained at a high number density, thus preventing the dislocation motion. Also the Al_3Sc particles have modest coarsening rates at elevated temperatures, leading to the effective suppression of recrystallization and the stabilization of microstructures at high temperatures. Thus Sc-containing Al-Mg alloys are expected to be used in higher-temperature application compared to conventional structural Al alloys.

In previous study [4], we examined the cyclic deformation behavior and dislocation microstructure under plastic-strain-controlled conditions at 423 K, using an aged Al-Mg-Sc alloy with Al_3Sc particles of different diameters, i.e. 4, 6 and 11 nm, which correspond to under-age, peak-age and over-age conditions, respectively. The over-aged alloy showed cyclic hardening to saturation. On the other hand, cyclic softening occurred in the under-aged and peak-aged alloys. Transmission electron microscopy (TEM) observation revealed that the 6 and 11 nm Al_3Sc particles have a stronger retardation effect on the formation of fatigue-induced stable dislocation structure than 4 nm particles at 423 K.

To establish a multifunctional method for fatigue life assessments, it is very useful to know the similarities and differences between stress- and strain-controlled fatigue behaviors. In this study, a polycrystalline Al-Mg-Sc alloy with dispersed Al_3Sc particles is cyclically deformed at an elevated temperature of 423K under various constant stress amplitudes, and the dislocation structure is investigated in relation to the stress-strain responses. As in the previous study [4], the two particle diameters of 4 and 11 nm have been selected.

Experimental procedure

Specimens for fatigue tests were cut from hot-rolled polycrystalline Al-1mass%Mg-0.27mass%Sc alloy plates with the stress axis parallel to the rolling direction. These specimens were solutionized at 905 K for 7.2 x 10^3 s and water quenched. TEM observations revealed that no precipitates existed in the solution treated specimens. To obtain spherical and coherent Al_3Sc particles, one set of solutionized specimens was aged at 573 K for 9.0 x 10^2 s, and second set was aged at 623 K for 6.48 x 10^4 s, corresponding to under-aging and over-aging conditions which produced almost the same Vickers hardness of 70. Hereafter, these under-aged and over-aged specimens will be referred to as specimens UA and OA, respectively. The average diameter of Al_3Sc particles in specimens UA was 4 nm, while the particle diameter in specimen OA averaged 11 nm. The average size was determined from TEM observations of over 200 particles. In addition another set of solution-treated specimens underwent a two-step aging treatment, that is, aging at 573 K for 3.0 x 10^2, water quenching, and then aging at 623 K for 6.48 x 10^4 s. This two-step aging produced Al_3Sc particles with the same diameter of 11nm. The two-step-aged specimen will be referred to as specimen OA2. Judging from the Al-Sc equilibrium phase diagram [5], the volume fractions of the Al_3Sc particles in specimens UA, OA and OA2 are nearly identical and are estimated as 0.007.

All mechanical tests were carried out at 423K in air. Tensile properties were determined with an initial strain rate of 3.0 x 10^{-3} s^{-1}. Fully-reversed tension-compression fatigue tests were performed under stress-amplitude control. The ramp loading method [6] was adopted and the ramp loading length was set to 30 cycles. A low frequency of 0.5 Hz was employed when the tests were started and the frequency was increased up to 10 Hz after several tens of cycles. The stress-strain hysteresis loops were monitored with a digital oscilloscope.

The fatigued specimens were sliced into 3mm disks parallel to the stress axis and were mechanically ground down to 0.2 mm. Thin foils for TEM observations were prepared by electro-polishing. Microscopy was performed with JOEL-2000EX and JOEL-2010FEF microscopes operating at 200 kV.

Results and Discussion

Mechanical Properties. The solutionized and aged specimens were coarse-grained with an equiaxed grain size of 0.5 to 1 mm. The Al-Mg-Sc ternary equilibrium phase diagram [7] shows that Mg in the present Al-1mass%Mg-0.27mass%Sc alloy does not form any compounds at the aging temperatures examined. In fact, aging of the alloy at 573 and 623 K produced only spherical Al_3Sc particles in the Al matrix.

Table 1 summarizes the tensile properties of specimens UA and OA tested at 423 K. For comparison, the results obtained at RT are also indicated. At 423 K, the values of 0.2% proof stress of the specimens UA and OA are almost the same. The values of 0.2% proof stress and tensile stress of both the specimens are smaller than those obtained at RT, while the values of fracture strain of specimens show a reverse tendency.

Table 1 Tensile properties of specimens UA, OA and OA2 obtained at 423 K and room temperature (RT).

Specimen	0.2% proof stress (MPa)		Tensile stress (MPa)		Fracture elongation (%)	
	423 K	RT	423 K	RT	423 K	RT
UA	127	130	150	170	24	21
OA	121	125	147	174	27	21
OA2	118	125	143	172	29	24

Fatigue tests under stress-amplitude control were performed at 423 K under stress amplitude control condition. The cyclic-deformation curves of specimens OA and UA are shown in Figs. 1 (a) and (b), where the plastic strain amplitude ε_{pl} is plotted against the number of fatigue cycles (N). In the case of stress-controlled tests, the decrease of ε_{pl} against N means cyclic hardening, and the increase of ε_{pl} corresponds to cyclic softening. For comparison, the cyclic-deformation curves for specimens OA and UA obtained at RT are also indicated in Figs. 1 [8].

In the OA specimens, monotonic hardening can be seen. The ε_{pl} decreases rapidly with increasing N and finally reaches saturation at all applied stress amplitudes. In contrast, the cyclic deformation curves of specimens UA show initial hardening and then clear cyclic softening at all stress amplitudes. No crack was detected on the specimen surface, indicating that the cyclic softening in specimens UA is not caused by surface crack initiation. The difference in the fatigue behavior between the specimens OA and UA will be discussed bellow in terms of the difference in the size of the Al_3Sc particles.

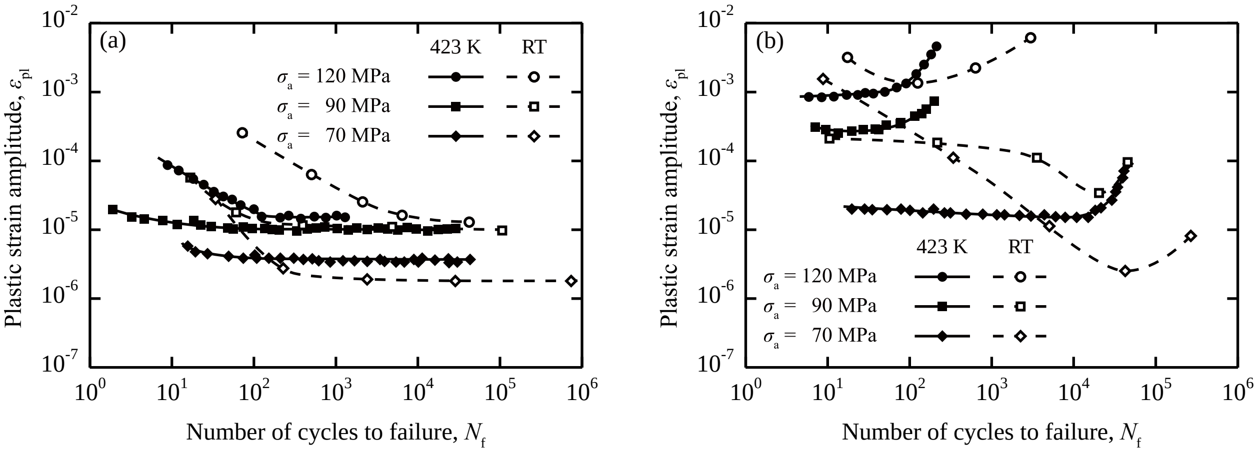

Fig. 1 Cyclic-deformation curves of specimens (a) OA and (b) UA obtained under various stress amplitudes σ_a. Also shown are the results obtained at RT [8].

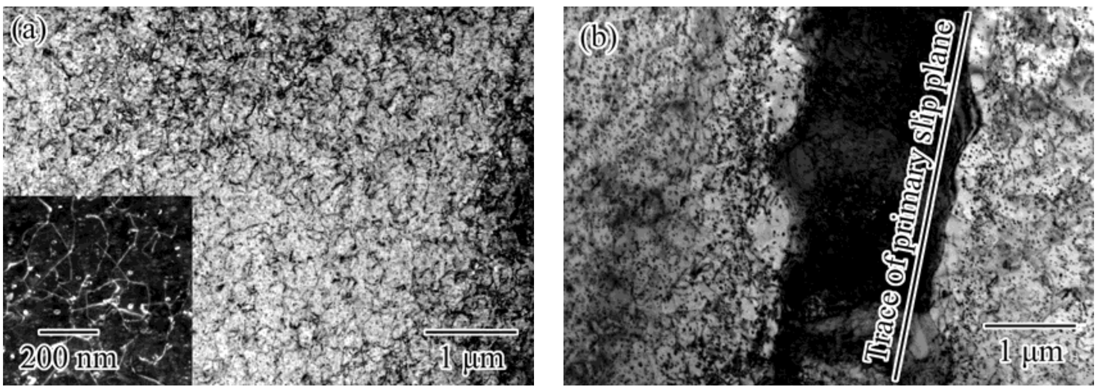

Fig. 2 TEM micrographs of specimens (a) OA and (b) UA fatigued under σ_a = 90 MPa. The inset in (a) is enlarged dark-field image.

Microstructures. Figures 2 (a) and (b) depict the typical fatigue dislocation microstructures formed at 423K under a applied stress amplitude σ_a of 90 MPa for specimens OA and UA. In the specimen OA, dislocations were uniformly distributed under all applied stress amplitudes, whereas the specimen UA, in which cyclic softening occurred in Fig. 1(b), exhibited clearly developed slip bands along the trace of primary slip plane. These slip bands indicate the occurrence of very inhomogeneous deformation. In other words, strong strain localization took place within the slip bands. Such strong strain localization usually causes the destruction and re-dissolution of particles [9]. To check whether shearing of Al_3Sc particles occurred during fatigue tests at 423 K, the average size of the Al_3Sc particles within slip bands or in the matrix was measured by TEM using a specimen UA re-aged at 623K for 6.48 x 10^4 s following a fatigue test to failure. The resulting average diameters were about 9 nm within the slip bands and 12 nm in the matrix. This discrepancy in the particle size implies that the small Al_3Sc particles of 4 nm were cut by moving dislocation within the strongly strained slip bands. The cyclic softening in specimen UA in fig. 1 (b) can then be explained by a decrease in particle strengthening through particle shearing or re-dissolution within the slip bands.

Fatigue Life. The results of fatigue life tests (*S*-*N* curves) for specimens UA and OA are shown in Fig. 3, where σ_a is plotted as a function of the number of cycles to failure (N_f). Since slip bands are known as sites for crack initiation, as would be expected, the specimen OA shows more enhanced fatigue life than the specimen UA.

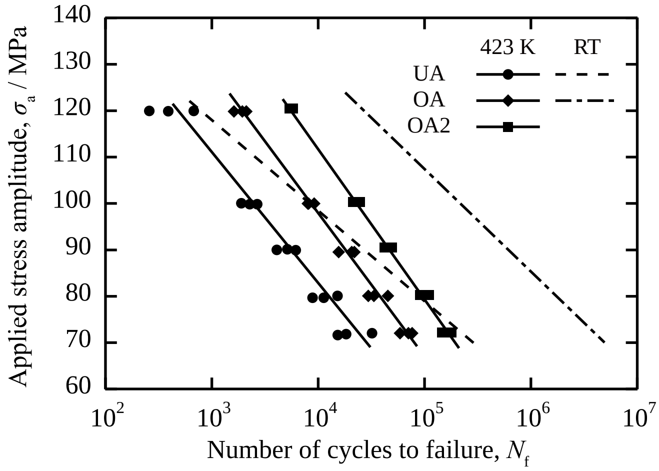

Fig. 3 *S*-*N* curves for specimens OA, UA and OA2 obtained at 423 K. The results for specimens OA and UA obtained at RT are also indicated [8].

In the specimen OA, precipitate-free zones (PFZs) were formed near the grain boundaries, and the averaged PFZs width was about 200 nm. In the addition to the difference in Al_3Sc particle sizes as mentioned above, the existence of PFZs can be pointed out as another factor affecting fatigue life. These PFZs have a low yield stress in comparison with the grain interior, thus favoring dislocation movement, and eventually crack nucleation seems to occur within the PFZs. In fact, the macroscopic cracks nucleated and propagated predominantly along the grain boundaries in the specimen OA, but the crack nucleation in the specimen UA occurred almost exclusively along the slip bands. Thus, It can be said that the existence of PFZs has a detrimental influence on the fatigue life of specimen OA.

The tensile properties of specimen OA2, two-step aged at 573 K for 3.0 x 10^2 s and then at 423 K for 6.48 x 10^4s, are summarized in Table 1. The two-step aging did not essentially change the Al_3Sc particles size and the strength but does increases the elongation. Also, the width of PFZs was reduced from 200 nm to 110 nm by the two-step aging. Comparison between the *S*-*N* curves of specimens OA and OA2 in Fig. 3 shows that the two-step aging results in enhanced fatigue life. Therefore we conclude that the decrease in the PFZ width brings about the increase in the fatigue life.

Summary

Stress amplitude controlled fatigue tests of Al-Mg-Sc alloy polycrystals with Al_3Sc particles of 4 and 11 nm in diameter were performed at 423 K. The results and conclusions are summarized as follows.

(1) Specimens UA bearing 4 nm Al_3Sc particles show cyclic softening, while specimen OA with 11 nm Al_3Sc particles show cyclic hardening to saturation.

(2) In the specimens UA, slip band dislocation structures are observed, and, in the specimen OA, dislocations are uniformly distributed.

(3) The cyclic softening of specimen UA is caused by shearing of small Al_3Sc particles within the slip bands.

(5) Two-step aging brings about reduction in the width of precipitate-free zones in the specimen with large particles and, as a result, it enhanced the fatigue life of the specimen.

Acknowledgement

This work was financially supported in part by The Light Metal Educational Foundation, Inc. The authors wish to acknowledge Furukawa SKY Aluminum Ltd. for supplying the alloys.

References

[1] M. Y. Drits, L. B. Ber, Y. G. Bykov, L. S. Toropova, G. K. Anastaseva, Aging of Al-0.3at.%Sc alloy, Phys. Met. Metall, 57 (1984) 118-126.

[2] R. R. Sawtell, C. L. Jensen, Mechanical properties and microstructures of Al-Mg-Sc alloys, Metall. Mater. Trans. A, 21 (1990) 421-430.

[3] V. I. Elagin, V. V. Zakharov, T. D. Rostova, Scandium-alloyed aluminum alloys, Met. Sci. Heat Treat., 34 (1992) 37-45.

[4] C. Watanabe, R. Monzen, Fatigue behavior and microstructure of an Al-Mg-Sc alloy at an elevated temperature, J. Physics: Conf. Series, 240 (2010) 012049.

[5] J. L. Murray, The Al-Sc (aluminum-scandium) system, J. Phase Equilib., 19 (1998) 380-384.

[6] L. Llanes, C. Laird, Substructure evolution of copper polycrystals under different testing conditions: conventional strain control and ramp loading, Mater. Sci. Eng. A, 161 (1993) 1-12.

[7] P. Villars, A. Prince, H. Okamoto, Handbook of ternary alloy phase diagrams, ASM, Materials Park, 1995, pp. 3900-3902.

[8] C. Watanabe, R. Monzen, K. Tazaki, Effects of Al_3Sc particle size and precipitate-free zones on fatigue behavior and dislocation structure of an aged Al-Mg-Sc alloy, Int. J. Fatigue, 30 (2008), 635-641.

[9] C. Calabrese, C. Laird, Cyclic stress—strain response of two-phase alloys Part I. Microstructures containing particles penetrable by dislocations, Mater. Sci. Eng. 13 (1974) 141-157.